

Submit to “Communications in Physics”, (0), pp. 1-0  
 DOI:10.15625/0868-3166/0/0/0

## ONE-LOOP OFF-SHELL DECAY $H^* \rightarrow ZZ$ AT FUTURE COLLIDERS

KHIEM HONG PHAN, DZUNG TRI TRAN

*Institute of Fundamental and Applied Sciences, Duy Tan University, Ho Chi Minh City 700000, Vietnam*

*Faculty of Natural Sciences, Duy Tan University, Da Nang City 550000, Vietnam*

ANH THU NGUYEN

*University of Science Ho Chi Minh City, 227 Nguyen Van Cu, District 5, Ho Chi Minh City, Vietnam*

*E-mail:* phanhongkhiem@duytan.edu.vn

*Received 9 May 2023*

*Accepted for publication DD MM YYYY*

**Abstract.** We present one-loop formulas for contributing to the  $HZZ$  vertex in 't Hooft-Veltman gauge within Standard Model framework. One-loop off-shell Higgs decay rates to  $Z$ -pair are investigated in both unpolarized and longitudinal polarization for  $Z$  bosons in final state. The corrections are range of 7% to 8.4% when we vary the off-shell Higgs mass from 200 GeV to 500 GeV. In applications, we study off-shell Higgs decay  $H^* \rightarrow ZZ$  in the Higgs productions at future colliders such as the signal processes  $\gamma^*(Q^2)\gamma \rightarrow H^* \rightarrow ZZ$  and  $e^-\gamma \rightarrow e^-H^* \rightarrow e^-ZZ$  are analyzed.

**Keyword:** One-loop corrections, Analytic methods for Quantum Field Theory, Dimensional regularization, Higgs phenomenology.

### I. Introduction

Since the discovery of the Standard-Model-like (SM-like) Higgs boson at the Large Hadron Collider (LHC) [1, 2], High energy physics have entered a new era. High-precision measurements of the Higgs properties are the top priority tasks at the LHC. So far, most of the measurements at the LHC focus on the on-shell Higgs productions and on-shell Higgs decay channels. The data shows that the Higgs signal strengths are in agreement with the SM predictions. The above measurements are planned to probe as precisely as possible in near future for the high-precision tests of the SM as well as extracting new physics beyond the SM (BSM). Besides that, in order to explore the nature of Higgs sector at different energy scales, off-shell Higgs decay channels are considerable interests. Recently, off-shell Higgs decay  $H^* \rightarrow Z^*Z^* \rightarrow 4$  leptons have been measured at the LHC in Refs. [3–8].

We argue that off-shell Higgs decay channel  $H^* \rightarrow ZZ \rightarrow 4$  leptons provides rich of phenomenological investigations. In Ref. [9], examining the tail of off-shell Higgs decay mode  $H^* \rightarrow Z_L Z_L$ , one can test the unitarity of the SM and explore new physics through high energy behavior. Searching for new physics through off-shell Higgs decay  $H^* \rightarrow ZZ \rightarrow l^+ l^- \nu_l \bar{\nu}_l$  has been studied in Ref. [10] in which the authors have considered the effective theory by proposing the energy-dependence operators. Off-Shell Higgs decays as a probe of naturalness have been discussed in Ref. [11] and as a probe of the trilinear Higgs coupling have been reported in Ref. [12]. Through the examination of the decay channel  $H \rightarrow ZZ^* \rightarrow 4$  leptons at the LHC, the authors in Ref. [13] have been studied the effects of the CP-conserving and CP-violating of the general  $HZZ$  coupling. Other phenomenological studies of off-shell Higgs decay in many of BSMs have been found in Refs. [14–20].

At the LHC, one-loop and two-loop QCD corrections for both signal and background of the off-shell Higgs decay  $H^* \rightarrow ZZ$  have been computed in [21–30]. One-loop electroweak corrections to Higgs boson decay into  $ZZ$  in standard model have been reported in [31], in the minimal supersymmetric model [32, 33], and to Higgs boson decay into four leptons have been evaluated in Refs. [34–36]. Off-shell Higgs decay effects in Higgs productions at future linear colliders have been studied in Refs. [37, 38] in which the authors have been included only the tree level vertex  $HZZ$  in the analysis. Due to the important roles of the off-shell Higgs decays and in order to match the high-precision data at future colliders, we evaluate for one-loop electroweak corrections to the off-shell decay  $H^* \rightarrow ZZ$  in this work. The computation is performed in 't Hooft-Veltman gauge. Analytic formulas for one-loop form factors in the decay process are expressed in terms of Passarino-Veltman scalar functions in the standard notations of LoopTools. As a result, the off-shell decay rates can be evaluated numerically by using this package. One-loop electroweak corrections to the off-shell decay rates are studied for the cases of unpolarized  $Z$  bosons and longitudinal polarization of  $Z$  bosons in final state. In applications, we study off-shell Higgs decay  $H^* \rightarrow ZZ$  in the Higgs productions at future colliders such as the signal processes  $\gamma^*(Q^2)\gamma \rightarrow H^* \rightarrow ZZ$  and  $e^-\gamma \rightarrow e^- H^* \rightarrow e^- ZZ$  are analyzed.

The layout of the paper is as follows: In section 2, we present one-loop expressions for the vertex  $HZZ$ . Phenomenological results for this work are shown in the section 3. Conclusions and outlook for this research are discussed in the section 4.

## II. Calculations

In general, one-loop contributions to the  $H(p)Z(q_1)Z(q_2)$  vertex are decomposed in terms of Lorentz structure as follows:

$$\mathcal{V}_{HZZ}^{1\text{-loop}}(p, q_1, q_2) = g_{HZZ} \left( F_{00} g^{\mu\nu} + \sum_{i,j=1}^2 F_{ij} q_i^\mu q_j^\nu \right). \quad (1)$$

The tree level coupling of the Higgs to  $ZZ$  is given  $g_{HZZ} = \frac{eM_W}{c_W^2 s_W}$  where  $s_W$  and  $c_W$  are sine and cosine of Weinberg angle respectively. In this expression, the terms  $F_{00}$ ,  $F_{ij}$  for  $i, j = 1, 2$  are denoted for one-loop form factors. These form factors are functions of  $p^2, q_1^2, q_2^2$  and they are expressed in terms of Passarino-Veltman scalar functions (called as PV-functions hereafter). All one-loop Feynman diagrams contributing to this vertex can be grouped into three classes as follows (shown in appendix D). By considering all fermions exchanging in the loop diagrams, this is

corresponding to group 1. With including all  $W$  bosons, goldstone bosons and ghost particles propagating in the loop, we have group 2 accordingly. One finally takes  $Z$  boson, Higgs and goldstone bosons exchanging in the loop, we have correspondingly to group 3. It is known that one-loop contributing to the vertex  $HZZ$  contains ultraviolet divergent ( $UV$ -divergent). Following renormalization theory, the counter-terms are given for cancelling the  $UV$ -divergent. We then have counter-term diagrams in group 0 which their analytic formulas are presented in appendix C.

Analytic results for the above form factors are computed class by class of Feynman diagrams as follows. First, one-loop amplitudes for all Feynman diagrams mentioned in above are written down. We then handle with Dirac traces and Lorentz contractions in  $d$  dimensions by using Package-X [39]. The amplitudes are next decomposed into tensor one-loop integrals. By following tensor reduction for one-loop integrals in [40], the tensor integrals are then expressed in terms of the PV-functions which they can be evaluated numerically by using LoopTools [41]. In detail, analytical results for all form factors are shown in the following paragraphs. General expression for the form factor  $F_{00}(p^2; q_1^2, q_2^2)$  is written as follows:

$$F_{00}(p^2; q_1^2, q_2^2) = \sum_{G=\{G_0, G_1, \dots, G_3\}} F_{00}^{(G)}(p^2; q_1^2, q_2^2). \quad (2)$$

Where  $\{G_0, G_1, \dots, G_3\} = \{\text{group 0, group 1}, \dots, \text{group 3}\}$  are groups of Feynman diagrams showing in appendix D. The form factor  $F_{00}^{(G_0)}(p^2; q_1^2, q_2^2)$  for group 0 is expressed in the appendix C. In group 1, we consider all fermions exchanging in the loop. We take top quark in the loop for an example. The resulting for the form factor reads:

$$\begin{aligned} F_{00}^{(G_1)}(p^2; q_1^2, q_2^2) &= \frac{e^3}{576\pi^2 M_W s_W^3 c_W^2} N_t^C m_t^2 \times \\ &\times \left\{ 2(32s_W^4 - 24s_W^2 + 9)B_0(p^2, m_t^2, m_t^2) + 9[B_0(q_1^2, m_t^2, m_t^2) + B_0(q_2^2, m_t^2, m_t^2)] \right. \\ &+ [36m_t^2 + 8s_W^2(3 - 4s_W^2)(-p^2 + q_1^2 + q_2^2) - 9(q_1^2 + q_2^2)]C_0(p^2, q_1^2, q_2^2, m_t^2, m_t^2, m_t^2) \\ &\left. - 8(32s_W^4 - 24s_W^2 + 9)C_{00}(p^2, q_1^2, q_2^2, m_t^2, m_t^2, m_t^2) \right\}. \end{aligned} \quad (3)$$

Here  $N_t^C = 3$  is color number top quark. For group 2, we take into account all  $W$  boson in the loop diagrams. The form factor is then given:

$$\begin{aligned} F_{00}^{(G_2)}(p^2; q_1^2, q_2^2) &= \frac{e^3}{64\pi^2 M_W s_W^3 c_W^2} \times \\ &\quad \times \left\{ 4M_W^2(c_W^4 - s_W^4) [B_0(q_1^2, M_W^2, M_W^2) + B_0(q_2^2, M_W^2, M_W^2)] \right. \\ &\quad - 4M_W^2 [c_W^4 (5p^2 - 4(q_1^2 + q_2^2 + M_W^2)) + s_W^2 c_W^2 (q_1^2 + q_2^2 - 2(p^2 + M_W^2))] \\ &\quad + s_W^4 (2M_W^2 + M_H^2) C_0(p^2, q_1^2, q_2^2, M_W^2, M_W^2, M_W^2) \\ &\quad + [4M_H^2(c_W^2 - s_W^2)^2 + 8M_W^2(c_W^4(4d - 7) - 2c_W^2 s_W^2 + s_W^4)] \times \\ &\quad \quad \quad \times C_{00}(p^2, q_1^2, q_2^2, M_W^2, M_W^2, M_W^2) \\ &\quad \left. - [8M_W^2 c_W^2 (c_W^2(d - 2) - s_W^2) + M_H^2(c_W^2 - s_W^2)^2] B_0(p^2, M_W^2, M_W^2) \right\}. \end{aligned} \quad (4)$$

We next consider the contributions from group 3 in which the particles  $Z, \chi_3, H$  are exchanged in the loop diagrams. The form factor is evaluated accordingly:

$$\begin{aligned} F_{00}^{(G_3)}(p^2; q_1^2, q_2^2) &= -\frac{e^3}{128\pi^2 M_W s_W^3 c_W^6} \left\{ 4c_W^2 M_W^2 [B_0(q_1^2, M_H^2, M_Z^2) + B_0(q_2^2, M_H^2, M_Z^2)] \right. \\ &\quad + 3M_H^2 C_0(p^2, q_1^2, q_2^2, M_H^2, M_H^2, M_Z^2) \\ &\quad + M_H^2 c_W^4 B_0(p^2, M_Z^2, M_Z^2) + 3c_W^4 M_H^2 B_0(p^2, M_H^2, M_H^2) \\ &\quad + 8M_W^4 C_0(p^2, q_1^2, q_2^2, M_Z^2, M_Z^2, M_H^2) - 12M_H^2 c_W^4 C_{00}(p^2, q_1^2, q_2^2, M_H^2, M_H^2, M_Z^2) \\ &\quad \left. - 4c_W^2 (c_W^2 M_H^2 + 2M_W^2) C_{00}(p^2, q_1^2, q_2^2, M_Z^2, M_Z^2, M_H^2) \right\}. \end{aligned} \quad (5)$$

Other form factors ( $F_{ij}$  for  $i, j = 1, 2$ ) are also written in the form of

$$F_{ij}(p^2; q_1^2, q_2^2) = \sum_{G=\{G_1, \dots, G_3\}} F_{ij}^{(G)}(p^2; q_1^2, q_2^2). \quad (6)$$

All form factors  $F_{ij}$  for  $i, j = 1, 2$  are the UV-finite. Therefore, we have only group 1 to group 3 contributing to these form factors. Applying the same procedure, each form factor is expressed as follows:

$$\begin{aligned} F_{11}^{(G_1)}(p^2; q_1^2, q_2^2) &= -\frac{e^3 (32s_W^4 - 24s_W^2 + 9)}{144\pi^2 M_W s_W^3 c_W^2} N_t^C m_t^2 \times \\ &\quad \times [C_1(p^2, q_1^2, q_2^2, m_t^2, m_t^2, m_t^2) + 2C_{11}(p^2, q_1^2, q_2^2, m_t^2, m_t^2, m_t^2)], \end{aligned} \quad (7)$$

$$\begin{aligned}
F_{11}^{(G_2)}(p^2; q_1^2, q_2^2) = & \frac{e^3}{32\pi^2 M_W s_W^3 c_W^2} \times \\
& \times \left\{ \left[ M_H^2 (c_W^2 - s_W^2)^2 + M_W^2 (2c_W^4 (4d - 7) - 3c_W^2 s_W^2 + 3s_W^4) \right] \times \right. \\
& \quad \times C_1(p^2, q_1^2, q_2^2, M_W^2, M_W^2, M_W^2) \\
& + \left[ 2M_H^2 (c_W^2 - s_W^2)^2 + 4M_W^2 (c_W^4 (4d - 7) - 2c_W^2 s_W^2 + s_W^4) \right] \times \\
& \quad \times C_{11}(p^2, q_1^2, q_2^2, M_W^2, M_W^2, M_W^2) \\
& \left. + 2M_W^2 s_W^2 (s_W^2 - 2c_W^2) C_0(p^2, q_1^2, q_2^2, M_W^2, M_W^2, M_W^2) \right\}, 
\end{aligned} \tag{8}$$

$$\begin{aligned}
F_{11}^{(G_3)}(p^2; q_1^2, q_2^2) = & \frac{e^3}{64\pi^2 M_W s_W^3 c_W^4} \left\{ 2M_W^2 C_0(p^2, q_1^2, q_2^2, M_Z^2, M_Z^2, M_H^2) \right. \\
& + (c_W^2 M_H^2 + 3M_W^2) C_1(p^2, q_1^2, q_2^2, M_Z^2, M_Z^2, M_H^2) \\
& + 3c_W^2 M_H^2 \left[ C_1(p^2, q_1^2, q_2^2, M_H^2, M_H^2, M_Z^2) + 2C_{11}(p^2, q_1^2, q_2^2, M_H^2, M_H^2, M_Z^2) \right] \\
& \left. + 2(c_W^2 M_H^2 + 2M_W^2) C_{11}(p^2, q_1^2, q_2^2, M_Z^2, M_Z^2, M_H^2) \right\}. 
\end{aligned} \tag{9}$$

Analytic results for the form factors  $F_{12}$  are shown as:

$$\begin{aligned}
F_{12}^{(G_1)}(p^2; q_1^2, q_2^2) = & -\frac{e^3}{288\pi^2 M_W s_W^3 c_W^2} N_t^C m_t^2 \left\{ 8s_W^2 (3 - 4s_W^2) C_0(p^2, q_1^2, q_2^2, m_t^2, m_t^2, m_t^2) \right. \\
& - (3 - 8s_W^2)^2 \left[ C_1(p^2, q_1^2, q_2^2, m_t^2, m_t^2, m_t^2) + C_1(p^2, q_2^2, q_1^2, m_t^2, m_t^2, m_t^2) \right] \\
& \left. - 4(32s_W^4 - 24s_W^2 + 9) C_{12}(q_1^2, p^2, q_2^2, m_t^2, m_t^2, m_t^2) \right\}, 
\end{aligned} \tag{10}$$

$$\begin{aligned}
F_{12}^{(G_2)}(p^2; q_1^2, q_2^2) = & \frac{e^3}{64\pi^2 M_W s_W^3 c_W^2} \left\{ \left[ 4M_W^2 (3s_W^2 c_W^2 + s_W^4 - 2c_W^4 (d - 2)) - M_H^2 (c_W^2 - s_W^2)^2 \right] \right. \\
& \times C_0(p^2, q_1^2, q_2^2, M_W^2, M_W^2, M_W^2) \\
& + \left[ M_H^2 (c_W^2 - s_W^2)^2 + M_W^2 (2c_W^4 (4d - 9) - 11c_W^2 s_W^2 - s_W^4) \right] \times \\
& \quad \times \left[ C_1(p^2, q_2^2, q_1^2, M_W^2, M_W^2, M_W^2) - 2C_1(p^2, q_1^2, q_2^2, M_W^2, M_W^2, M_W^2) \right] \\
& - 4 \left[ M_H^2 (c_W^2 - s_W^2)^2 + 2M_W^2 (c_W^4 (4d - 7) - 2s_W^2 c_W^2 + s_W^4) \right] \\
& \quad \times C_{12}(q_1^2, p^2, q_2^2, M_W^2, M_W^2, M_W^2) \left. \right\}, 
\end{aligned} \tag{11}$$

$$\begin{aligned}
F_{12}^{(G_3)}(p^2; q_1^2, q_2^2) = & \frac{e^3}{128\pi^2 M_W s_W^3 c_W^4} \left\{ (4M_W^2 - c_W^2 M_H^2) C_0(p^2, q_1^2, q_2^2, M_Z^2, M_Z^2, M_H^2) \right. \\
& - 3c_W^2 M_H^2 C_0(p^2, q_1^2, q_2^2, M_H^2, M_H^2, M_Z^2) \\
& - 6c_W^2 M_H^2 \left[ C_1(p^2, q_1^2, q_2^2, M_H^2, M_H^2, M_Z^2) + C_1(p^2, q_2^2, q_1^2, M_H^2, M_H^2, M_Z^2) \right. \\
& \quad \left. \left. + 2C_{12}(q_1^2, p^2, q_2^2, M_Z^2, M_H^2, M_H^2) \right] \right. \\
& + \left( 2M_W^2 - 2c_W^2 M_H^2 \right) \left[ C_1(p^2, q_1^2, q_2^2, M_Z^2, M_Z^2, M_H^2) + C_1(p^2, q_2^2, q_1^2, M_Z^2, M_Z^2, M_H^2) \right] \\
& \left. - 4(2M_W^2 + c_W^2 M_H^2) C_{12}(q_1^2, p^2, q_2^2, M_H^2, M_Z^2, M_Z^2) \right\}.
\end{aligned} \tag{12}$$

We list all analytic expressions for the form factor  $F_{21}$  as follows:

$$\begin{aligned}
F_{21}^{(G_1)}(p^2; q_1^2, q_2^2) = & -\frac{e^3}{288\pi^2 M_W s_W^3 c_W^2} N_t^C m_t^2 \times \\
& \times \left\{ 8s_W^2 (4s_W^2 - 3) C_0(p^2, q_1^2, q_2^2, m_t^2, m_t^2, m_t^2) - 9 \left[ C_1(p^2, q_1^2, q_2^2, m_t^2, m_t^2, m_t^2) \right. \right. \\
& \quad \left. \left. + C_1(p^2, q_2^2, q_1^2, m_t^2, m_t^2, m_t^2) \right] - 4(32s_W^4 - 24s_W^2 + 9) C_{12}(q_1^2, p^2, q_2^2, m_t^2, m_t^2, m_t^2) \right\},
\end{aligned} \tag{13}$$

$$\begin{aligned}
F_{21}^{(G_2)}(p^2; q_1^2, q_2^2) = & -\frac{e^3}{16\pi^2 M_W s_W^3 c_W^2} \left\{ \left[ M_H^2 (c_W^2 - s_W^2)^2 + 2M_W^2 \left( c_W^4 (4d - 7) + s_W^2 (s_W^2 - 2c_W^2) \right) \right] \right. \\
& \times C_{12}(q_1^2, p^2, q_2^2, M_W^2, M_W^2, M_W^2) \\
& + 2M_W^2 \left[ C_1(p^2, q_1^2, q_2^2, M_W^2, M_W^2, M_W^2) + C_1(p^2, q_2^2, q_1^2, M_W^2, M_W^2, M_W^2) \right] \\
& \left. + 8M_W^2 c_W^2 (s_W^2 - c_W^2) C_0(p^2, q_1^2, q_2^2, M_W^2, M_W^2, M_W^2) \right\},
\end{aligned} \tag{14}$$

$$\begin{aligned}
F_{21}^{(G_3)}(p^2; q_1^2, q_2^2) = & -\frac{e^3}{32\pi^2 M_W s_W^3 c_W^4} \times \\
& \times \left\{ 2M_W^2 \left[ C_1(p^2, q_1^2, q_2^2, M_Z^2, M_Z^2, M_H^2) + C_1(p^2, q_2^2, q_1^2, M_Z^2, M_Z^2, M_H^2) \right] \right. \\
& + (c_W^2 M_H^2 + 2M_W^2) C_{12}(q_1^2, p^2, q_2^2, M_H^2, M_Z^2, M_Z^2) \\
& \left. + 3c_W^2 M_H^2 C_{12}(q_1^2, p^2, q_2^2, M_Z^2, M_H^2, M_H^2) \right\}.
\end{aligned} \tag{15}$$

The last form factor  $F_{22}$  can be derived directly as

$$F_{22}(p^2; q_1^2, q_2^2) = F_{11}(p^2; q_2^2, q_1^2). \tag{16}$$

Moreover, it is easy to check that all form factors satisfy the Bose symmetry relations

$$F_{00,12,21}(p^2; q_1^2, q_2^2) = F_{00,12,21}(p^2; q_2^2, q_1^2). \quad (17)$$

We turn our attention to one-loop amplitude for off-shell  $H^* \rightarrow ZZ$ . In this case, we only have  $F_{00}, F_{21}$  contributing to the amplitude. Analytic expressions for these form factors can be obtained by taking  $q_1^2 = q_2^2 = M_Z^2$ . One-loop off-shell decay rates for  $H^* \rightarrow ZZ, Z_L Z_L$  are computed. We use the following kinematic variables:  $p^2 = M_{ZZ}^2, q_1^2 = M_Z^2$  and  $q_2^2 = M_Z^2$ . Decay rate for the case of unpolarized  $Z$  bosons in final state gets the form of

$$\begin{aligned} \Gamma_{H^* \rightarrow ZZ} = & \frac{g_{HZZ}^2 \sqrt{\lambda(M_{ZZ}^2, M_Z^2, M_Z^2)}}{(64\pi)M_Z^4 M_{ZZ}^3} \left\{ \left( 12M_Z^4 - 4M_Z^2 M_{ZZ}^2 + M_{ZZ}^4 \right) + \right. \\ & + \left( 2M_{ZZ}^4 - 8M_Z^2 M_{ZZ}^2 + 24M_Z^4 \right) \Re e \left[ F_{00}(M_{ZZ}^2, M_Z^2, M_Z^2) \right] \\ & \left. + \left( 8M_Z^4 M_{ZZ}^2 - 6M_Z^2 M_{ZZ}^4 + M_{ZZ}^6 \right) \Re e \left[ F_{21}(M_{ZZ}^2, M_Z^2, M_Z^2) \right] \right\}. \end{aligned} \quad (18)$$

Here, the Källén function is defined as  $\lambda(x; y, z) = (x - y - z)^2 - 4yz$ .

We next consider the polarized  $Z$  bosons. In rest frame of Higgs boson, the longitudinal polarization vectors for  $Z$  bosons are defined as:

$$\epsilon_\mu(q_i, \lambda = 0) = \frac{4M_{ZZ}^2 q_{i,\mu} - 2M_Z^2 p_\mu}{M_Z \sqrt{\lambda(4M_{ZZ}^2, M_Z^2, M_Z^2)}}, \quad \text{for } i = 1, 2. \quad (19)$$

By deriving again the squared amplitude for off-shell decay  $H^* \rightarrow Z_L Z_L$ , we then arrive at

$$\begin{aligned} \Gamma_{H^* \rightarrow Z_L Z_L} = & \frac{g_{HZZ}^2 \sqrt{\lambda(M_{ZZ}^2, M_Z^2, M_Z^2)}}{(2\pi)M_Z^4 M_{ZZ}^3 \lambda^2(4M_{ZZ}^2, M_Z^2, M_Z^2)} \left\{ 2M_{ZZ}^4 \left( M_Z^4 - 6M_Z^2 M_{ZZ}^2 + 2M_{ZZ}^4 \right)^2 + \right. \\ & + M_{ZZ}^4 \left( M_Z^4 - 6M_Z^2 M_{ZZ}^2 + 2M_{ZZ}^4 \right) \times \\ & \times \left[ \left( 4M_Z^4 - 24M_Z^2 M_{ZZ}^2 + 8M_{ZZ}^4 \right) \Re e \left[ F_{00}(M_{ZZ}^2, M_Z^2, M_Z^2) \right] \right. \\ & \left. \left. + \left( 25M_Z^4 M_{ZZ}^2 - 20M_Z^2 M_{ZZ}^4 + 4M_{ZZ}^6 \right) \Re e \left[ F_{21}(M_{ZZ}^2, M_Z^2, M_Z^2) \right] \right] \right\}. \end{aligned} \quad (20)$$

### III. Phenomenological results

In the phenomenological results, we use  $M_Z = 91.1876$  GeV,  $\Gamma_Z = 2.4952$  GeV,  $M_W = 80.379$  GeV,  $\Gamma_W = 2.085$  GeV,  $M_H = 125$  GeV,  $\Gamma_H = 4.07 \cdot 10^{-3}$  GeV. The lepton masses are given:  $m_e = 0.00052$  GeV,  $m_\mu = 0.10566$  GeV and  $m_\tau = 1.77686$  GeV. For quark masses, one takes  $m_u = 0.00216$  GeV,  $m_d = 0.0048$  GeV,  $m_c = 1.27$  GeV,  $m_s = 0.93$  GeV,  $m_t = 173.0$  GeV, and

$m_b = 4.18$  GeV. We work in the so-called  $G_\mu$ -scheme in which the Fermi constant is taken  $G_\mu = 1.16638 \cdot 10^{-5}$  GeV $^{-2}$  and the electroweak coupling can be calculated appropriately as follows:

$$\alpha = \sqrt{2}/\pi G_\mu M_W^2 (1 - M_W^2/M_Z^2) = 1/132.184. \quad (21)$$

We then present the phenomenological results in the following subsections. In Fig. 1, off-shell Higgs decay rates as a function of  $M_{ZZ}$  are shown. We vary  $M_{ZZ}$  from 200 GeV to 500 GeV. In the left (right) panel of Fig. 1, the decay rates are generated in the region of  $200 \leq M_{ZZ} \leq 500$  GeV (and zoom out in  $200 \leq M_{ZZ} \leq 300$  GeV to study the effects of  $H^* \rightarrow Z_L Z_L$ ), respectively. In these figures, the solid line presents for tree-level decay rates, the dashed line shows for full one-loop electroweak decay rates. While the dash-dotted line is for full one-loop decay rates with the longitudinal polarization for Z bosons. We find that the decay rates in  $H^* \rightarrow Z_L Z_L$  give small contributions in the low region of  $M_{ZZ}$  and they tend to one-loop decay rates in high region of  $M_{ZZ}$ .

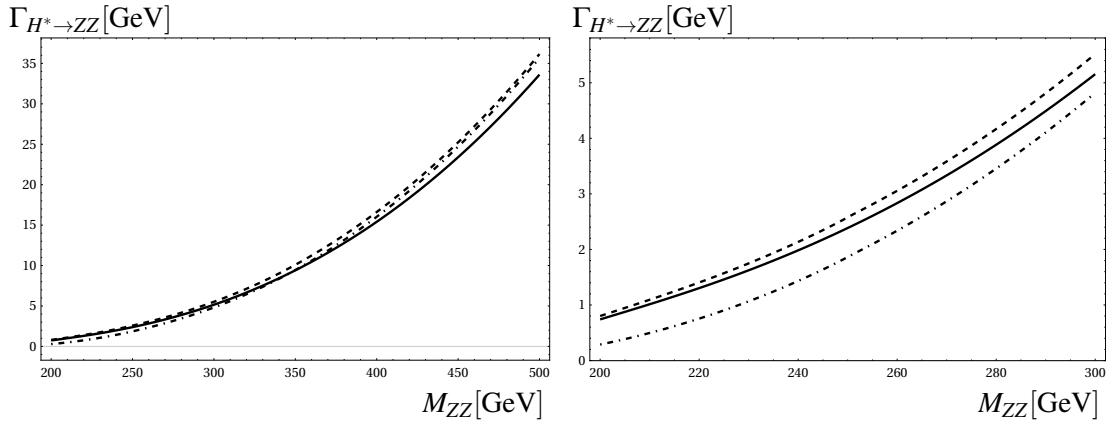


**Fig. 1.** Off-shell Higgs decay rates as a function of  $M_{ZZ}$ .

In Fig. 2, we show one-loop electroweak corrections to the decay rates. The corrections are defined as follows:

$$\delta[\%] = \frac{\Gamma_{H^* \rightarrow ZZ}^{\text{one-loop}} - \Gamma_{H^* \rightarrow ZZ}^{\text{tree}}}{\Gamma_{H^* \rightarrow ZZ}^{\text{tree}}} \times 100\%. \quad (22)$$

In the left panel, one presents one-loop corrections for the case of unpolarized bosons in final state. While the right figure shows for one-loop electroweak corrections for the case of longitudinal polarization for both Z bosons. We find that the corrections are in range of 7% to 8.4% for the case of unpolarized bosons. While the corrections change from  $-60\%$  to  $+10\%$  in the case of longitudinal polarization for both Z bosons. The effects of one-loop electroweak corrections to off-shell Higgs decay  $H^* \rightarrow ZZ$  are significant and they should be taken into account at future colliders.

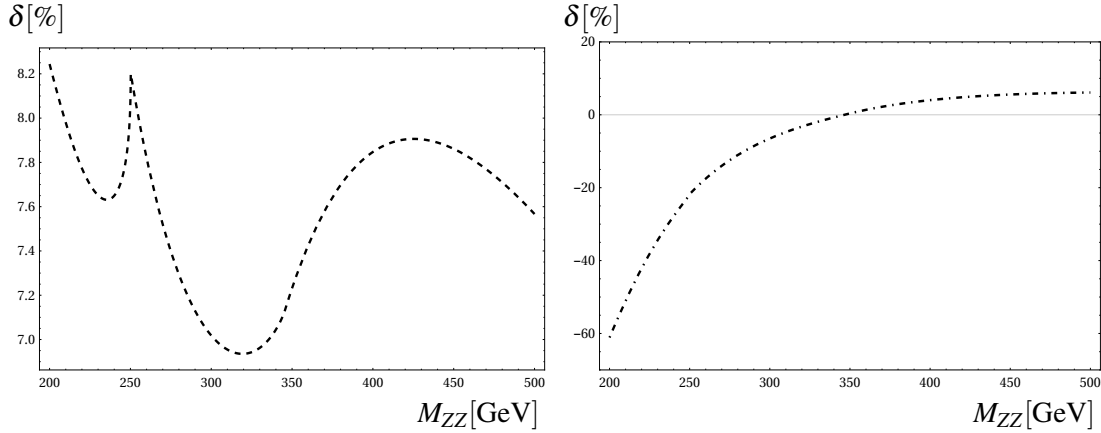


**Fig. 2.** One-loop electroweak corrections to the decay rates as a function of  $M_{ZZ}$ .

We study the effects of one-loop off-shell  $H^* \rightarrow ZZ$  in Higgs productions at future colliders. The first signal process is  $\gamma(Q^2)\gamma \rightarrow H^* \rightarrow ZZ$ . The signal cross section is given by

$$\sigma(\sqrt{s}, Q^2) = \frac{2\sqrt{s} \Gamma_{H^* \rightarrow ZZ}}{[(s - M_H^2)^2 + \Gamma_H^2 M_H^2] \sqrt{\lambda(s, Q^2, 0)}} |F_{00}^{H^* \rightarrow \gamma^*\gamma}(s, Q^2, 0)|^2. \quad (23)$$

Where  $F_{00}^{H^* \rightarrow \gamma^*\gamma}(s, Q^2, 0)$  is one-loop form factor for process  $H^* \rightarrow \gamma^*(Q^2)\gamma$  which its analytical result can be found in [46]. In Fig. 3, total cross sections are plotted as a function of center-of-mass energy (C.o.M) for  $Q^2 = 0$  (left panel) and  $Q^2 = 1.5M_H^2$  (right panel) respectively. In these Figures, the solid line shows for tree-level cross sections, the dashed line is for one-loop contributing to  $H^* \rightarrow ZZ$  and the dash-dotted line presents for one-loop contributing to  $H^* \rightarrow Z_L Z_L$ .

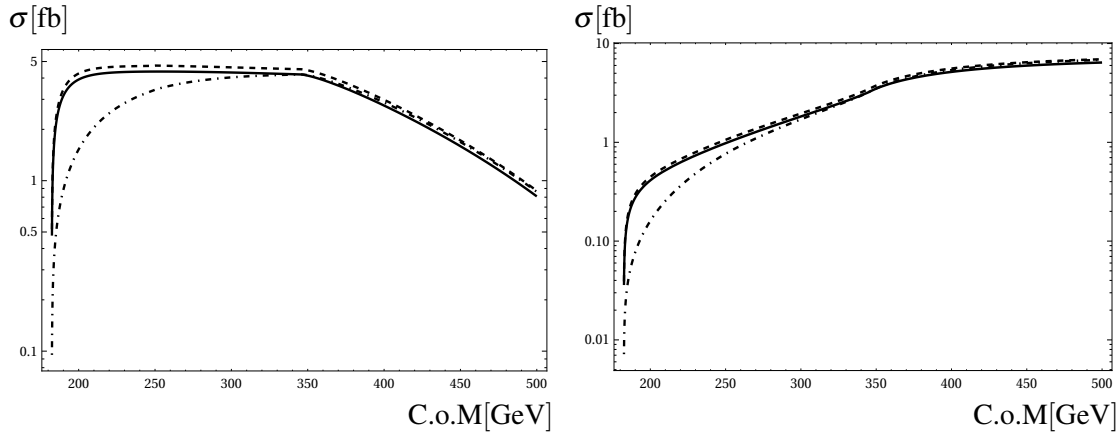


**Fig. 3.** Total cross sections are plotted as a function of center-of-mass energy (C.o.M) for  $Q^2 = 0$  (left panel) and  $Q^2 = 1.5M_H^2$  (right panel) respectively.

The second signal process mentioned in this work is  $e^-\gamma \rightarrow e^-H^* \rightarrow e^-ZZ$ . The signal cross section is written as follows

$$\begin{aligned} \frac{d^2\sigma(\sqrt{s}, Q^2)}{dM_{ZZ} dQ^2} &= \frac{e^2}{16\pi s} \left[ \frac{s^2 + (M_{ZZ}^2 - Q^2 - s)^2}{Q^2(s^2 - Q^2)^2} \right] \times \left| F_{00}^{H^*\rightarrow\gamma^*\gamma}(s, Q^2, 0) \right|^2 \times \\ &\quad \times \frac{2M_{ZZ}}{[(M_{ZZ}^2 - M_H^2)^2 + \Gamma_H^2 M_H^2]} \times \frac{M_{ZZ} \Gamma_{H^*\rightarrow ZZ}(M_{ZZ})}{\pi}. \end{aligned} \quad (24)$$

In Fig. 4, we present differential cross sections with respect to off-shell Higgs mass  $M_{ZZ}$  (left panel) and  $Q^2$  (right panel). In these distributions, we use the same previous notations. In the left Figure, cross section develops to the peak which is corresponding to  $M_{ZZ} \sim 2M_Z$ . It then decrease rapidly beyond the peak. It is interesting to observe that one-loop off-shell Higgs decay impacts are visible around the peak. In the right Figure, we find that cross section is dominant in the low  $Q^2$  regions.

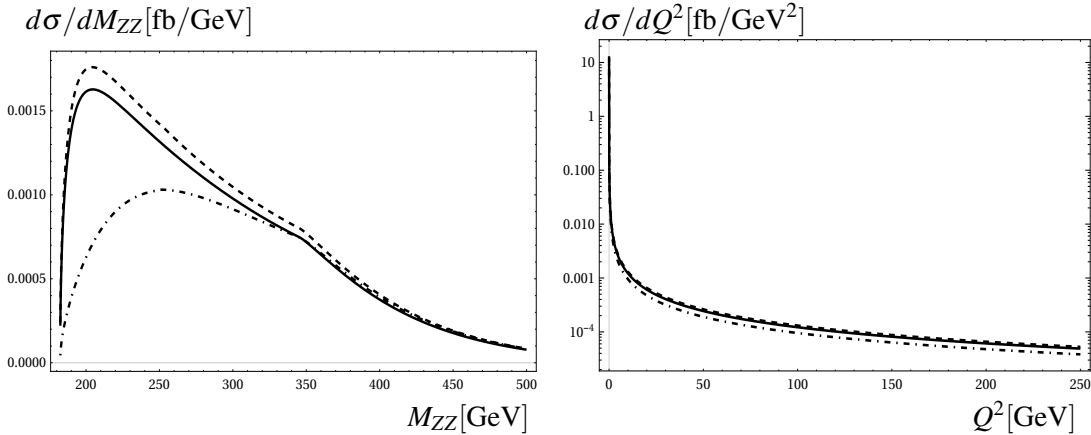


**Fig. 4.**

In both cases, one finds that the effects of one-loop contributions to off-shell Higgs decay to Z-pair are visible and they should be taken into account at future colliders.

#### IV. Conclusions

In this paper, we have performed one-loop electroweak contributing to  $HZZ$  vertex in 't Hooft-Veltman gauge. We have also presented one-loop formulas for off-shell decay  $H^* \rightarrow ZZ, Z_L Z_L$ . Analytic expressions for one-loop form factors are shown in terms of the PV-functions in the standard notations of `LoopTools`. Therefore, off-shell decay rates can be computed numerically by using this package. One-loop electroweak corrections to the off-shell decay rates are investigated for the cases of unpolarized  $Z$  bosons and longitudinal polarization of  $Z$  bosons in final state. The corrections are range of 7% to 8.4% when varying off-shell Higgs mass  $200 \text{ GeV} \leq M_{ZZ} \leq 500 \text{ GeV}$ . In applications, we study off-shell Higgs decay  $H^* \rightarrow ZZ$  in the Higgs productions at future colliders such as the signal processes  $\gamma^*(Q^2)\gamma \rightarrow H^* \rightarrow ZZ$  and  $e^-\gamma \rightarrow e^-H^* \rightarrow e^-ZZ$  are studied. We find that the effects of one-loop contributions to off-shell

Higgs decay to  $Z$ -pair are visible and they should be taken into account at future colliders.

**Acknowledgment:** This research is funded by Vietnam National University, Ho Chi Minh City (VNU-HCM) under grant number C2022-18-14.

## Appendix A: Checks for the calculation

Before representing the phenomenological results, we are going to check the  $UV$ -finiteness of the results. As we mentioned in the previous section, the form factors  $F_{00}^{(G_j)}$  for  $j = 1, 2, 3$  contain the  $UV$ -divergent. By taking the counter-term form factor  $F_{00}^{(G_0)}$ , the total form factor  $F_{00}$  is then  $UV$ -finite. The numerical results for this check are presented in the following Table 1. By changing  $C_{UV}, \mu^2$ , we verify that the total form factor  $F_{00}$  is very good stability (over 11 digits).

$(C_{UV}, \mu^2)$	$\sum_{j=1}^3 F_{00}^{(G_j)}$ $F_{00}^{(G_0)}$ $F_{00} = \sum_{j=0}^3 F_{00}^{(G_j)}$
$(0, 1)$	$-13.315051817147474 + 2.5760460657959703 i$ $16.425138633496918 + 0 i$ $3.110086816349444 + 2.5760460657959703 i$
$(10^2, 10^4)$	$137.93892691326275 + 2.5760460657959703 i$ $-134.82884009691335 + 0 i$ $3.110086816349394 + 2.5760460657959703 i$
$(10^4, 10^8)$	$13861.982684608432 + 2.5760460657959703 i$ $-13858.872597792075 + 0 i$ $3.1100868163575797 + 2.5760460657959703 i$

**Table 1.** Checking for the  $UV$ -finiteness of the results at  $M_{ZZ} = 250$  GeV ( $p^2 = M_{ZZ}^2$ ). In this case, two real bosons are considered in final state.

## Appendix B: Decay width of off-shell $H^* \rightarrow ZZ^* \rightarrow Zl\bar{l}$ and $H^* \rightarrow Z^*Z^* \rightarrow l_1\bar{l}_1l_2\bar{l}_2$ with $l_{1,2} = e, \mu, \nu_e, \nu_\mu, \nu_\tau$

We also include the leptons decay from  $Z$  boson. Since we are interested in the off-shell Higgs decay to  $ZZ$ . It means that  $p_H^2 \geq 4M_Z^2$ . Consequently, one can apply resonant approximation.

The decay rates for  $H \rightarrow ZZ^* \rightarrow Zl\bar{l}$  can be then presented in a compact form as:

$$\begin{aligned} \Gamma_{H \rightarrow Z^*Z \rightarrow Zl\bar{l}} &= \int_{\frac{4m_l^2}{M_Z^2}}^{(M_{ZZ}-M_Z)^2} \frac{dq_1^2}{\pi} \frac{M_Z \Gamma_Z^l}{(q_1^2 - M_Z^2)^2 + M_Z^2 \Gamma_Z^2} \frac{g_{HZZ}^2 \sqrt{\lambda(M_{ZZ}^2, q_1^2, M_Z^2)}}{(64\pi) M_Z^3 M_{ZZ}^3 q_1^2} \times \\ &\times \left\{ \left[ M_Z^4 - 2M_Z^2(M_{ZZ}^2 - 5q_1^2) + (M_{ZZ}^2 - q_1^2)^2 \right] \right. \\ &+ \left[ 2M_Z^4 - 4M_Z^2(M_{ZZ}^2 - 5q_1^2) + 2(M_{ZZ}^2 - q_1^2)^2 \right] \Re e \left[ F_{00}(M_{ZZ}^2, q_1^2, M_Z^2) \right] \\ &- \left( M_Z^2 - M_{ZZ}^2 + q_1^2 \right) \times \\ &\left. \left[ M_Z^4 - 2M_Z^2(M_{ZZ}^2 + q_1^2) + (M_{ZZ}^2 - q_1^2)^2 \right] \Re e \left[ F_{21}(M_{ZZ}^2, q_1^2, M_Z^2) \right] \right\}. \end{aligned} \quad (25)$$

Where  $M_Z \Gamma_Z^l = \frac{M_Z g^2 s_W^2 (a_l^2 + v_l^2)}{12\pi}$  is partial decay rate of  $Z$  to lepton pair with  $a_l = T_3^f / (2s_W c_W)$  and  $v_l = (T_3^f - 2Q_f s_W^2) / (2s_W c_W)$ . Following zero width approximation (ZWA) for  $Z$  decay into leptons, we employ

$$\frac{1}{(q_1^2 - M_Z^2)^2 + M_Z^2 \Gamma_Z^2} \rightarrow \frac{\pi}{M_Z \Gamma_Z} \delta(q_1^2 - M_Z^2). \quad (26)$$

One then has

$$\int_{\frac{4m_l^2}{M_Z^2}}^{(M_{ZZ}-M_Z)^2} dq_1^2 \delta(q_1^2 - M_Z^2) = 1. \quad (27)$$

As a result, we arrive at

$$\Gamma_{H \rightarrow Z^*Z \rightarrow Zl\bar{l}} = \Gamma_{H \rightarrow ZZ} \times \text{BR}_{Z \rightarrow l\bar{l}}. \quad (28)$$

We next consider leptons decay from both  $Z$  bosons. Applying the resonant approximation, one-loop off-shell decay rates  $H^* \rightarrow Z^*Z^* \rightarrow l_1\bar{l}_1l_2\bar{l}_2$  read:

$$\begin{aligned} \Gamma_{H \rightarrow Z^*Z^* \rightarrow 4 \text{ leptons}} = & \int_{4m_{l_1}^2}^{M_{ZZ}^2} \frac{dq_1^2}{\pi} \frac{M_Z \Gamma_Z^{l_1}}{(q_1^2 - M_Z^2)^2 + M_Z^2 \Gamma_Z^2} \int_{4m_{l_2}^2}^{(M_{ZZ}-\sqrt{q_1^2})^2} \frac{dq_2^2}{\pi} \frac{M_Z \Gamma_Z^{l_2}}{(q_2^2 - M_Z^2)^2 + M_Z^2 \Gamma_Z^2} \\ & \times \frac{g_{HZZ}^2 \sqrt{\lambda(M_{ZZ}, q_1^2, q_2^2)}}{(64\pi) M_Z^2 M_{ZZ}^3 q_1^2 q_2^2} \left\{ \left[ M_{ZZ}^4 - 2M_{ZZ}^2(q_1^2 + q_2^2) + q_1^4 + 10q_1^2 q_2^2 + q_2^4 \right] \right. \\ & + \left[ 2M_{ZZ}^4 - 4M_{ZZ}^2(q_1^2 + q_2^2) + 2q_1^4 + 20q_1^2 q_2^2 + 2q_2^4 \right] \mathcal{R}e \left[ F_{00}(M_{ZZ}, q_1^2, q_2^2) \right] \\ & + \left( M_{ZZ}^2 - q_1^2 - q_2^2 \right) \times \\ & \left. \times \left[ M_{ZZ}^4 - 2M_{ZZ}^2(q_1^2 + q_2^2) + (q_1^2 - q_2^2)^2 \right] \mathcal{R}e \left[ F_{21}(M_{ZZ}, q_1^2, q_2^2) \right] \right\}. \end{aligned} \quad (29)$$

With the help of ZWA, we arrive at

$$\Gamma_{H \rightarrow Z^*Z^* \rightarrow Zl_1\bar{l}_1l_2\bar{l}_2} = \Gamma_{H \rightarrow ZZ} \times \text{Br}_{Z \rightarrow l_1\bar{l}_1} \times \text{Br}_{Z \rightarrow l_2\bar{l}_2}. \quad (30)$$

### Appendix C: Counter-term for the vertex $HZZ$

Counter-term for the  $HZZ$  vertex has general form as follows [44]:

$$F_{00}^{(G_0)}(p^2; q_1^2, q_2^2) = (\delta Y + \delta G_2 + \delta G_3 + \delta G_Z + 2\delta Z_{ZZ}^{1/2} + \delta Z_H^{1/2}) \langle ZZH \rangle, \quad (31)$$

where  $\langle ZZH \rangle$  will refer to the tree-level expression of the above vertex. All renormalization constants can be found in [44, 47].

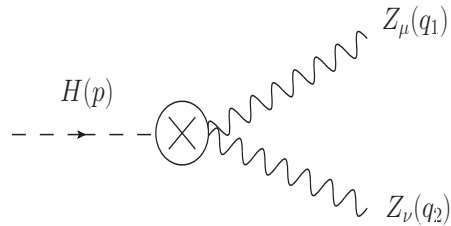


**Fig. 5.** Group 0: counter-term Feynman diagram.

### Appendix D: Feynman diagrams

#### REFERENCES

- [1] G. Aad *et al.* [ATLAS], Phys. Lett. B **716** (2012), 1-29 doi:10.1016/j.physletb.2012.08.020 [arXiv:1207.7214 [hep-ex]].
- [2] S. Chatrchyan *et al.* [CMS], Phys. Lett. B **716** (2012), 30-61 doi:10.1016/j.physletb.2012.08.021 [arXiv:1207.7235 [hep-ex]].

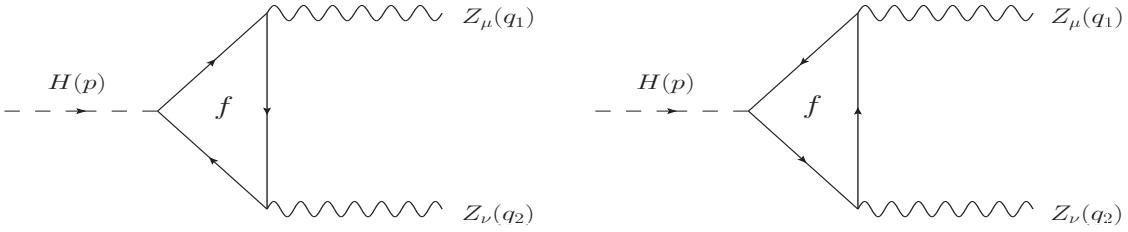


**Fig. 6.** one-loop Feynman diagrams with exchanging  $f$  in the loop (Group 1).

- [3] V. Khachatryan *et al.* [CMS], Phys. Lett. B **736** (2014), 64-85 doi:10.1016/j.physletb.2014.06.077 [arXiv:1405.3455 [hep-ex]].
- [4] G. Aad *et al.* [ATLAS], Eur. Phys. J. C **75** (2015) no.7, 335 doi:10.1140/epjc/s10052-015-3542-2 [arXiv:1503.01060 [hep-ex]].
- [5] G. Aad *et al.* [ATLAS], Eur. Phys. J. C **76** (2016) no.1, 45 doi:10.1140/epjc/s10052-015-3820-z [arXiv:1507.05930 [hep-ex]].
- [6] M. Aaboud *et al.* [ATLAS], Phys. Lett. B **786** (2018), 223-244 doi:10.1016/j.physletb.2018.09.048 [arXiv:1808.01191 [hep-ex]].
- [7] A. M. Sirunyan *et al.* [CMS], Phys. Rev. D **99** (2019) no.11, 112003 doi:10.1103/PhysRevD.99.112003 [arXiv:1901.00174 [hep-ex]].
- [8] [CMS], CMS-PAS-HIG-21-013.
- [9] S. J. Lee, M. Park and Z. Qian, Phys. Rev. D **100** (2019) no.1, 011702 doi:10.1103/PhysRevD.100.011702 [arXiv:1812.02679 [hep-ph]].
- [10] D. Gonçalves, T. Han, S. Ching Iris Leung and H. Qin, Phys. Lett. B **817** (2021), 136329 doi:10.1016/j.physletb.2021.136329 [arXiv:2012.05272 [hep-ph]].
- [11] D. Goncalves, T. Han and S. Mukhopadhyay, Phys. Rev. Lett. **120** (2018) no.11, 111801 [erratum: Phys. Rev. Lett. **121** (2018) no.7, 079902] doi:10.1103/PhysRevLett.120.111801 [arXiv:1710.02149 [hep-ph]].
- [12] U. Haisch and G. Koole, JHEP **02** (2022), 030 doi:10.1007/JHEP02(2022)030 [arXiv:2111.12589 [hep-ph]].
- [13] R. M. Godbole, D. J. Miller and M. M. Muhlleitner, JHEP **12** (2007), 031 doi:10.1088/1126-6708/2007/12/031 [arXiv:0708.0458 [hep-ph]].
- [14] A. Azatov, J. de Blas, A. Falkowski, A. V. Gritsan, C. Grojean, L. Kang, N. Kauer, E. Salvioni, U. Sarica and M. Thomas, *et al.* doi:10.17181/LHCCHWG-2022-001 [arXiv:2203.02418 [hep-ph]].
- [15] G. Cacciapaglia, A. Deandrea, G. Drieu La Rochelle and J. B. Filament, Phys. Rev. Lett. **113** (2014) no.20, 201802 doi:10.1103/PhysRevLett.113.201802 [arXiv:1406.1757 [hep-ph]].
- [16] H. E. Logan, Phys. Rev. D **92** (2015) no.7, 075038 doi:10.1103/PhysRevD.92.075038 [arXiv:1412.7577 [hep-ph]].
- [17] C. Englert, Y. Soreq and M. Spannowsky, JHEP **05** (2015), 145 doi:10.1007/JHEP05(2015)145 [arXiv:1410.5440 [hep-ph]].
- [18] Y. Chen, R. Harnik and R. Vega-Morales, JHEP **09** (2015), 185 doi:10.1007/JHEP09(2015)185 [arXiv:1503.05855 [hep-ph]].
- [19] D. Gonçalves, T. Han and S. Mukhopadhyay, Phys. Rev. D **98** (2018) no.1, 015023 doi:10.1103/PhysRevD.98.015023 [arXiv:1803.09751 [hep-ph]].
- [20] S. Dwivedi, D. K. Ghosh, B. Mukhopadhyaya and A. Shivaji, Phys. Rev. D **93** (2016), 115039 doi:10.1103/PhysRevD.93.115039 [arXiv:1603.06195 [hep-ph]].
- [21] F. Caola, J. M. Henn, K. Melnikov, A. V. Smirnov and V. A. Smirnov, JHEP **06** (2015), 129 doi:10.1007/JHEP06(2015)129 [arXiv:1503.08759 [hep-ph]].
- [22] F. Caola, K. Melnikov, R. Röntsch and L. Tancredi, Phys. Rev. D **92** (2015) no.9, 094028 doi:10.1103/PhysRevD.92.094028 [arXiv:1509.06734 [hep-ph]].
- [23] J. M. Campbell, R. K. Ellis, M. Czakon and S. Kirchner, JHEP **08** (2016), 011 doi:10.1007/JHEP08(2016)011 [arXiv:1605.01380 [hep-ph]].

- [24] F. Caola, M. Dowling, K. Melnikov, R. Röntsch and L. Tancredi, JHEP **07** (2016), 087 doi:10.1007/JHEP07(2016)087 [arXiv:1605.04610 [hep-ph]].
- [25] R. Gröber, A. Maier and T. Rauh, Phys. Rev. D **100** (2019) no.11, 114013 doi:10.1103/PhysRevD.100.114013 [arXiv:1908.04061 [hep-ph]].
- [26] J. Davies, G. Mishima, M. Steinhauser and D. Wellmann, JHEP **04** (2020), 024 doi:10.1007/JHEP04(2020)024 [arXiv:2002.05558 [hep-ph]].
- [27] S. Alioli, S. Ferrario Ravasio, J. M. Lindert and R. Röntsch, Eur. Phys. J. C **81** (2021) no.8, 687 doi:10.1140/epjc/s10052-021-09470-5 [arXiv:2102.07783 [hep-ph]].
- [28] M. Grazzini, S. Kallweit, M. Wiesemann and J. Y. Yook, Phys. Lett. B **819** (2021), 136465 doi:10.1016/j.physletb.2021.136465 [arXiv:2102.08344 [hep-ph]].
- [29] L. Buonocore, G. Koole, D. Lombardi, L. Rottoli, M. Wiesemann and G. Zanderighi, JHEP **01** (2022), 072 doi:10.1007/JHEP01(2022)072 [arXiv:2108.05337 [hep-ph]].
- [30] U. Haisch and G. Koole, JHEP **04** (2022), 166 doi:10.1007/JHEP04(2022)166 [arXiv:2201.09711 [hep-ph]].
- [31] B. A. Kniehl, Nucl. Phys. B **352** (1991), 1-26 doi:10.1016/0550-3213(91)90126-I.
- [32] D. Pierce and A. Papadopoulos, Phys. Rev. D **47** (1993), 222-231 doi:10.1103/PhysRevD.47.222 [arXiv:hep-ph/9206257 [hep-ph]].
- [33] W. Hollik and J. H. Zhang, Phys. Rev. D **84** (2011), 055022 doi:10.1103/PhysRevD.84.055022 [arXiv:1109.4781 [hep-ph]].
- [34] S. Boselli, C. M. Carloni Calame, G. Montagna, O. Nicrosini and F. Piccinini, JHEP **06** (2015), 023 doi:10.1007/JHEP06(2015)023 [arXiv:1503.07394 [hep-ph]].
- [35] A. Bredenstein, A. Denner, S. Dittmaier and M. M. Weber, Phys. Rev. D **74** (2006), 013004 doi:10.1103/PhysRevD.74.013004 [arXiv:hep-ph/0604011 [hep-ph]].
- [36] A. Bredenstein, A. Denner, S. Dittmaier and M. M. Weber, JHEP **02** (2007), 080 doi:10.1088/1126-6708/2007/02/080 [arXiv:hep-ph/0611234 [hep-ph]].
- [37] S. Liebler, G. Moortgat-Pick and G. Weiglein, JHEP **06** (2015), 093 doi:10.1007/JHEP06(2015)093 [arXiv:1502.07970 [hep-ph]].
- [38] B. Yan, Phys. Lett. B **822** (2021), 136709 doi:10.1016/j.physletb.2021.136709 [arXiv:2105.04530 [hep-ph]].
- [39] H. H. Patel, Comput. Phys. Commun. **197** (2015), 276-290 doi:10.1016/j.cpc.2015.08.017 [arXiv:1503.01469 [hep-ph]].
- [40] A. Denner and S. Dittmaier, Nucl. Phys. B **734** (2006), 62-115 doi:10.1016/j.nuclphysb.2005.11.007 [arXiv:hep-ph/0509141 [hep-ph]].
- [41] T. Hahn and M. Perez-Victoria, Comput. Phys. Commun. **118** (1999), 153-165 doi:10.1016/S0010-4655(98)00173-8 [arXiv:hep-ph/9807565 [hep-ph]].
- [42] N. Kauer and G. Passarino, JHEP **08** (2012), 116 doi:10.1007/JHEP08(2012)116 [arXiv:1206.4803 [hep-ph]].
- [43] K. i. Hikasa, Phys. Lett. B **164** (1985), 385 [erratum: Phys. Lett. B **195** (1987), 623] doi:10.1016/0370-2693(85)90346-6.
- [44] K. I. Aoki, Z. Hioki, M. Konuma, R. Kawabe and T. Muta, Prog. Theor. Phys. Suppl. **73** (1982), 1-225 doi:10.1143/PTPS.73.1.
- [45] G. Altarelli, B. Mele and F. Pitolli, Nucl. Phys. B **287** (1987), 205-224 doi:10.1016/0550-3213(87)90103-9.
- [46] K. H. Phan and D. T. Tran, Commun. in Phys. **32** (2022) no.1, 77 doi:10.15625/0868-3166/16022.
- [47] D. T. Tran and K. H. Phan, [arXiv:2211.15116 [hep-ph]].

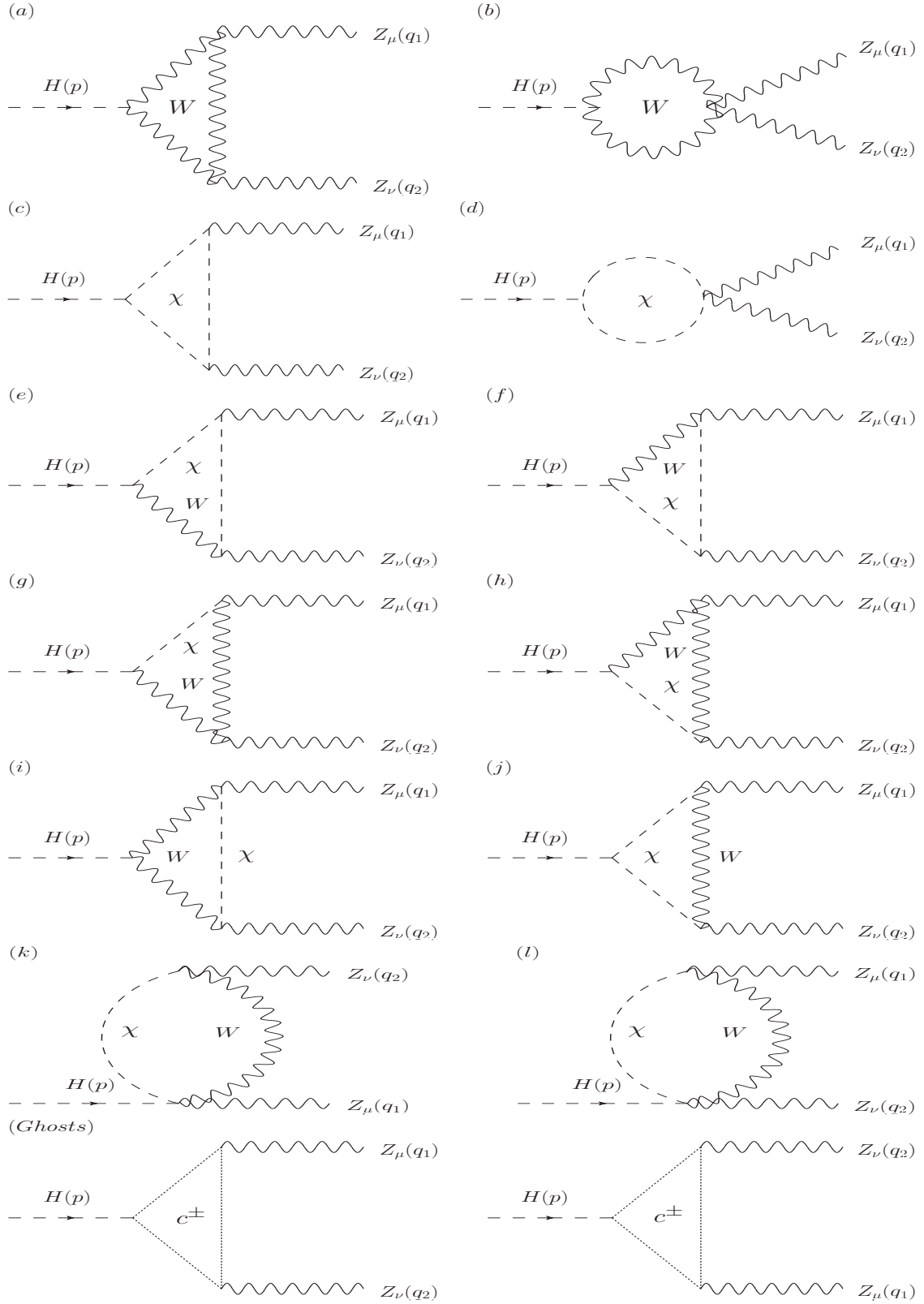


**Fig. 7.** one-loop Feynman diagrams with exchanging  $W, \chi$  and ghost particles in the loop (Group 2).

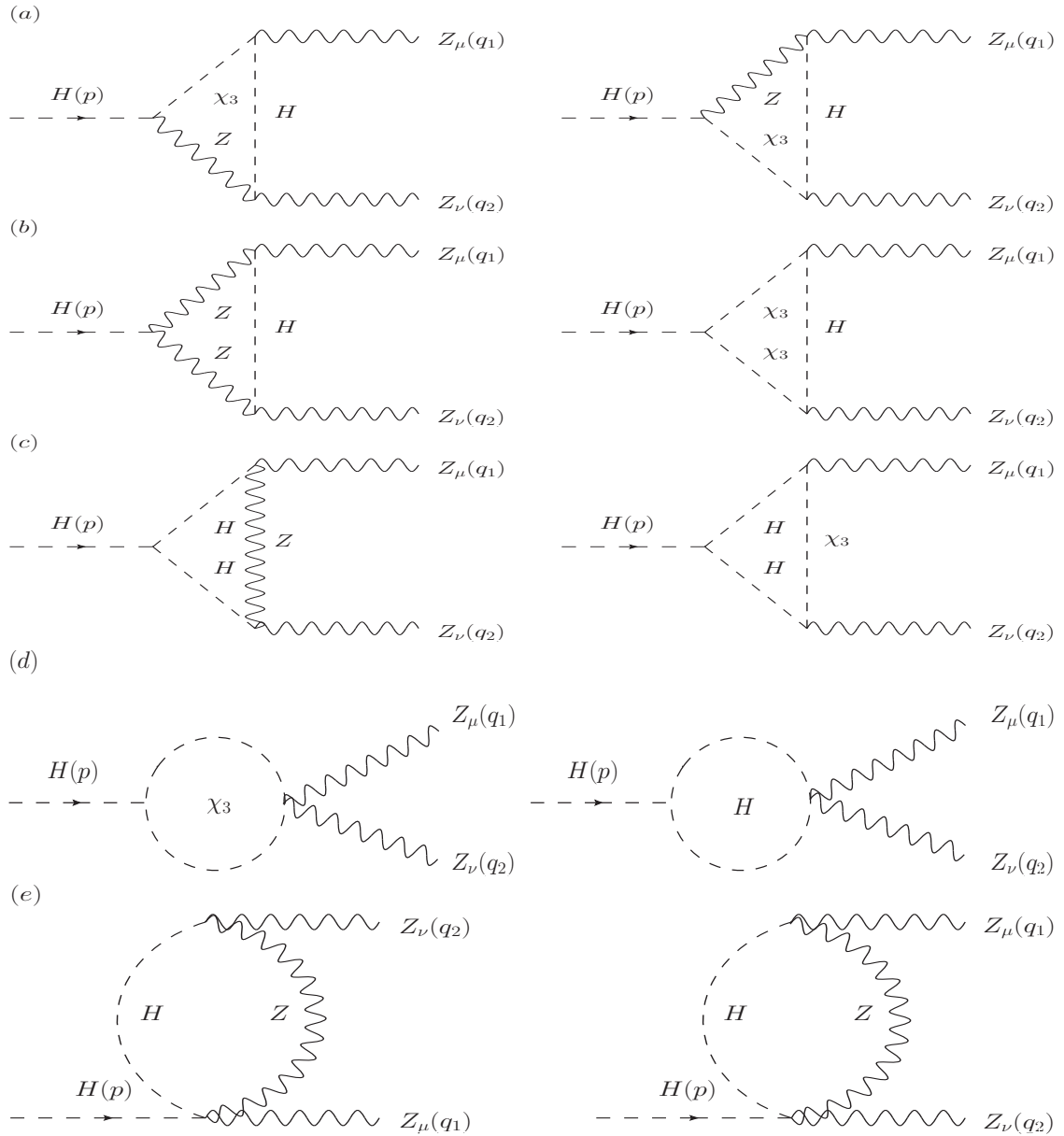


**Fig. 8.** one-loop Feynman diagrams with exchanging  $Z, \chi_3$  and  $H$  in the loop (Group 3).